Short-Term Hyperuricemia Leads to Structural Retinal Changes That Can be Reversed by Serum Uric Acid Lowering Agents in Mice

Hung-Liang Pai,[1] Sophie Meng-Tien Hsieh,[2] Yu-Shan Su,[3] Xin-Yuan Sue,[2] Han-Hsin Chang,[3] and David Pei-Cheng Lin[2,4]

[1]Department of Medicine, Chung Shan Medical University, Taichung, Taiwan, Republic of China
[2]Department of Medical Laboratory and Biotechnology, Chung Shan Medical University, Taichung, Taiwan, Republic of China
[3]Department of Nutrition, Chung Shan Medical University, Taichung, Taiwan, Republic of China
[4]Department of Ophthalmology, Chung Shan Medical University Hospital, Taichung, Taiwan, Republic of China

Correspondence: David Pei-Cheng Lin, No. 110, Sec. 1, Jianguo North Rd., Taichung City, Taiwan 40201, Republic of China;
pcl@csmu.edu.tw.
Han-Hsin Chang, No. 110, Sec. 1, Jianguo North Rd., Taichung City, Taiwan 40201, Republic of China;
jhhc@csmu.edu.tw.

PURPOSE. Metabolic disorders have been implicated in ocular diseases, such as age-related macular degeneration (AMD) and diabetic retinopathy (DR). Recently, hyperuricemia (HUA) has been proposed as another risk factor for AMD, although no cause-and-effect experimental data have been published. In this study, we investigated whether HUA would initiate AMD or related retinal damages in hyperuricemic mice.

METHODS. HUA was induced in male ICR mice by dietary supplements of uric acid and oxonic acid potassium salt, with or without treatments by allopurinol or benzbromarone for various durations. Serum uric acid and angiotensin II concentrations were measured by enzyme-linked immunosorbent assay (ELISA) at regular intervals. The retinal damages were assessed by hematoxylin and eosin staining, immunostaining, and TUNEL assay. The cause-and-effect of HUA was compared among the study groups.

RESULTS. The results showed that the total thickness of photoreceptor inner and outer segments, as well as the thickness of the photoreceptor outer segment alone, were reduced under HUA. Furthermore, HUA elevated serum angiotensin II, which indicated activation of the renin–angiotensin system (RAS), leading to higher matrix metalloproteinase-2 (MMP-2) expression, and glial activation in the ganglion cell layer. HUA also led to the reduction of retinal pigment epithelium gap junction protein connexin-43 and apoptosis. Uric acid lowering agents, allopurinol or benzbromarone, were effective in ameliorating the impairments.

CONCLUSIONS. HUA may pose as a causative factor of retinal injuries. The reduction of serum uric acid may reduce the detrimental effects caused by HUA.

Keywords: metabolic disorders, hyperuricemia, retinal injuries, allopurinol, benzbromarone

Currently, metabolic syndrome is a major challenge for public health, with increasing prevalence especially in the aging population.[1] Individuals with typical metabolic disorders, such as dyslipidemia, poor plasma glucose control, and high blood pressure, commonly manifest a pro-inflammatory state.[2] Several metabolic components have been well associated with ocular diseases, including cataract, diabetic retinopathy (DR), and age-related macular degeneration (AMD).[3] For example, deficiency in glucose tolerance and higher glycemic concentration are common risk factors for cataract.[4,5] Besides, hyperglycemia, hypertension, and insulin resistance have been reported to contribute in DR progression.[6] Furthermore, AMD progressing has been correlated to the status of obesity, high triglycerides, and high glucose.[7]

Hyperuricemia (HUA), another infliction of metabolic syndrome, is mostly known as a major risk factor for gout, especially when monosodium urate crystals are deposited in the joints.[8] Emerging evidence has suggested a link between HUA and ocular diseases through the inflammatory cascade of NLRP3 (NOD-, LRR-, and pyrin domain-containing protein 3) and subsequent pyroptosis attributed to reactive oxygen species (ROS) generation.[9] In addition, uric acid (UA) significantly increases the expression of angiotensin II (Ang II), one of the major components of the renin–angiotensin system (RAS), and subsequently affects the severity of retinopathy.[10,11] However, most of the evidence is derived from indirect data, in lack of experimental results to support the scenario of HUA-induced retinal damages.

Recently, we postulated a hypothesis that a new entity, "hyperuricemic AMD," may exist.[12] However, previous studies had contradictory conclusions in relating HUA as a pathogenic factor to AMD. One study proposed that HUA is

correlated with AMD only when choroidal neovascularization occurs.[13] In contrast, another cohort study of 1,684,314 subjects found that patients over 65 years old with gout were at higher risks of developing AMD, with a significant positive association.[14] In this study, we investigated whether HUA would initiate AMD or related retinal damages in hyperuricemic mice. We also examined the potential reversal effect by UA-lowering drugs, either allopurinol or benzbromarone. Our study provides a new aspect that HUA may play a crucial role in the process of retinal damage and related ocular diseases.

MATERIALS AND METHODS

Animals

Male ICR mice aged 28 weeks were purchased from the Bio-Lasco Taiwan Co., Ltd. (Taipei, Taiwan, Republic of China). The experimental mice were maintained in the Experimental Animal Center at Chung Shan Medical University in Taichung, Taiwan, Republic of China. The mice were housed and maintained in a controlled environment (temperature at $25 \pm 2°C$ and humidity at 50–75%, with a 12/12 hours light/dark cycle). The mice were acclimatized for 1 week before feeding an experimental diet prepared by combining oxonic acid potassium salt (OA; product No. 156124; Sigma-Aldrich, St. Louis, MO, USA) and UA (product No. U0881; Sigma-Aldrich; Fig. 1). The mice were randomly divided into six groups (all groups contained 6 mice, except the 5 for the control group): the control group (which received a standard diet), the low-dose group (1% UA with 2% OA), the medium-dose group (3% UA with 2% OA), the high-dose group (5% UA with 2% OA), the high-dose + allopurinol (HA) group (5% UA with 2% OA + allopurinol dissolved in water at 200 mg/L), and the high-dose + benzbromarone (HB) group (5% UA with 2% OA + benzbromarone dissolved in water at 15 mg/dL). The experimental diet lasted 8 weeks. Allopurinol (product No. A8003; Sigma-Aldrich) and benzbromarone (product No. B5774; Sigma-Aldrich) were orally administered each day starting from week 6. Bodyweight, serum uric acid (SUA), and serum Ang II were measured every 2 weeks. The animal study was reviewed and approved by the Institutional Animal Care and Use Committee of Chung Shan Medical University (No. 2383).

Enzyme-Linked Immunosorbent Assay for SUA and Serum Ang II Quantification

Blood samples were taken on day 1 and on the last day of weeks 4, 6, and 8. The SUA and Ang II were measured using a commercially available mouse Uric Acid Colorimetric Assay Kit (cat. No. E-BC-K016-M; Elabscience Biotechnology Co., Ltd.) and Mouse Angiotensin II ELISA Kit (cat. No. E-EL-M2612; Elabscience Biotechnology Co., Ltd.). Both protocols were conducted following the manufacturer's instructions.

Histopathological and Immunohistochemical Detection and Analyses

All mouse eyes were fixed in 10% neutral buffered formalin followed by standard embedding procedures in paraffin. Hematoxylin and eosin stains were conducted to investigate the eye sections under a light microscope (Leica M500-N). The thickness of photoreceptor inner segment and outer segment (OS/IS) and photoreceptor outer segment (PROS) was measured at 50 μm, 100 μm, 150 μm, and 200 μm intervals to the optic nerve head along the superior and inferior halves. SGcapture software (Optical Gaging Products)
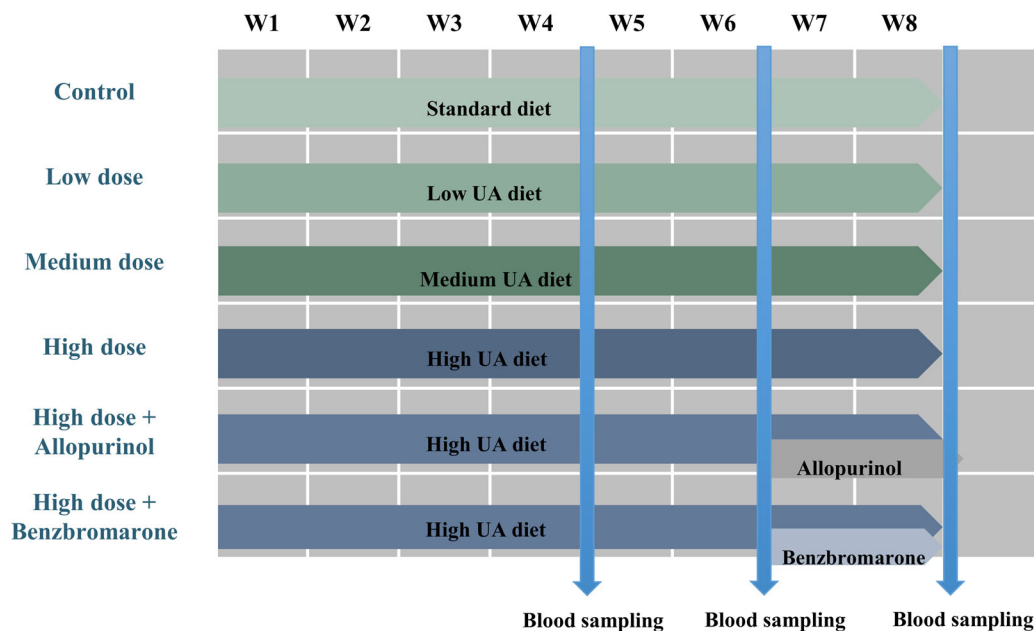

FIGURE 1. A diagram shows the timeline of the six study groups. The six study groups were: control group (standard diet), low-dose group (1% UA with 2% OA), medium-dose group (3% UA with 2% OA), high-dose group (5% UA with 2% OA), high-dose + allopurinol (HA) group (5% UA with 2% OA + allopurinol dissolved in water at 200 mg/L) and high-dose + benzbromarone (HB) group (5% UA with 2% OA + benzbromarone dissolved in water at 15 mg/dL). OA and UA were given as a mixture in the mouse food. Allopurinol and benzbromarone were orally administered daily after week 6. Blood samples for serum uric acid and angiotensin II measurements were taken on day 1 and on the last day of weeks 4, 6, and 8. OA, oxonic acid potassium salt; UA, uric acid.

was used to measure the OS/IS and PROS thickness in each defined position for every study group ($n = 6$). To minimize the artifact, the thickness was calculated by two different operators.

For antigen retrieval, eye sections were microwave-heated for 25 minutes with citrate buffer (pH = 6.0). Endogenous peroxidase blockage was performed by a 5% hydrogen peroxide solution, followed by immersion in a 1% bovine serum albumin (BSA) solution for 10 minutes to prevent nonspecific interactions. The primary matrix metalloproteinase-2 (MMP-2) antibodies (cat. No. NB200-193; Novus Biologicals, LLC) were diluted to 1:200 in a 1% solution of BSA and added to the tissue sections. These were kept at 4°C overnight in a humid box and washed 3 times with tris-buffered saline (TBS) buffer for 5 minutes. The secondary antibodies (cat. No. 305035003; Jackson ImmunoResearch Laboratories) were diluted to 1:200 with a 1% solution of BSA and added to the sections. These were immersed for 30 minutes and washed by TBS buffer at room temperature. For color detection, 3,3′-diaminobenzidine (DAB, 40 mg/dL; DAKO, USA) was incubated to the eye sections for 5 minutes. Then, the preparations were counterstained with hematoxylin, air-dried, and sealed by coverslips with mounting gels. The stains were observed and photographed under a microscope.

To detect immunofluorescence, connexin-43 (CX-43) primary antibody (cat. No. PA5-11632; Thermo Fisher Scientific) and glial fibrillary acidic protein (GFAP) primary antibody (cat. No. AB5541; Sigma-Aldrich) were diluted to 1:100 and 1:200 in 1% BSA solution, respectively. The primary antibodies were added to sections and kept under 4°C in a humid box overnight. The sections were then rinsed with TBS three times and incubated with a corresponding secondary antibody (Alexa Fluor 488; cat. No. AB150077; Abcam plc). DAPI (product No. D9542; Sigma-Aldrich) staining was performed for 5 minutes at room temperature to locate nucleoli. The preparations were viewed and photographed under a fluorescent microscope (Axio Imager A2; ZEISS) with activation/emission wavelengths of 358/463 nm for DAPI and 495/519 nm for FITC. The photographs were analyzed for fluorescence intensity using ImageJ (version 1.50f–an open-source image processing software).[15] The procedures were performed following the protocol in a previous study.[16] The identical adjustment was conducted before measuring the mean fluorescence intensity and comparing among different groups. For CX-43 and GFAP analysis, the RPE and retinal ganglion cells (RGCs) was selected as region of interests, respectively. All images were acquired with the same time exposure.

TUNEL Assay for Apoptosis of Retinal Pigment Epithelium

The retinal pigment epithelium (RPE) cells containing fragmented DNA were detected by terminal deoxynucleotidyl-transferase (TdT)-mediated deoxyuridine triphosphate-digoxigenin (dUTP) nick-end labeling (TUNEL). The TUNEL assay was performed with an in situ apoptosis detection kit (BioVision, Milpitas, CA, USA). Propidium iodide (PI) was used to stain nucleoli for 10 minutes at room temperature. Images of TUNEL and PI fluorescence were observed using the fluorescent microscope with activation/emission wavelength at 495/519 nm for FITC and at 538/617 nm for PI.

The ratios of TUNEL-positive RPE cells were calculated and presented in percentages.

Statistics

All statistical data were analyzed using the Statistical Package for Social Sciences (SPSS; SPSS Inc., Chicago, IL, USA) program version 15. Values are expressed as mean ± SD. Intergroup differences between time points were assessed for statistical significance using the Kruskal-Wallis test in the six groups. Once the test was significant, the single comparisons were performed by the Wilcoxon test. Significant difference was set at $P < 0.05$.

RESULTS

HUA Induction and Intervention by Allopurinol and Benzbromarone

After receiving the UA-added diet, the experimental groups showed significant elevation of UA concentration at different study periods (Fig. 2, Table 1). HUA was induced in the high-dose group starting from week 4 to week 8 ($P < 0.05$ in week 4, and $P < 0.01$ in both week 6 and 8, compared to the control group). This indicated the successful induction of HUA (see Fig. 2A). In the HA and HB groups, HUA were lasted for only 2 weeks (for the HA group, $P < 0.05$ in week 4 and week 6, compared to the control group; and for the HB group, $P < 0.05$ in week 4 and $P < 0.01$ in week 6, compared to the control group), and were suppressed significantly by UA-lowering treatments ($P < 0.01$ in both the HA and HB groups, compared to the high-dose group in week 8). Compared with the control group, significant differences were observed after week 6 and week 8 for the medium-dose group ($P < 0.05$ and $P < 0.01$, respectively), showing that a relative high concentration of SUA was maintained for 2 weeks (from week 6 to week 8). The SUA level in the low-dose group was significantly increased only in week 8 ($P < 0.05$), compared to the control group. There were no significant differences among the six groups in body weight (Supplementary Table S1).

RAS Activation as Reflected by Serum Ang II Elevation

To evaluate the influence of HUA on RAS activation, we assessed serum Ang II concentration using ELISA. With the UA-added diet, Ang II concentration was increased dose-dependently in the hyperuricemic mice (see Fig. 2B, Table 2). In line with HUA, significant higher Ang II concentration in the high-dose group was observed from week 4 to week 8 ($P < 0.01$ in weeks 4, 6, and 8, compared to the control group). In the HA and HB groups, higher Ang II were lasted for only 2 weeks (for the HA group, $P < 0.01$ in week 4 and week 6, compared to the control group; and for the HB group, $P < 0.01$ in week 4 and in week 6, compared to the control group), and were suppressed significantly by UA-lowering treatments ($P < 0.01$ in both the HA and HB groups, compared to the high-dose group in week 8). For the medium-dose group, significant differences were detected after week 6 and week 8 ($P < 0.05$ and $P < 0.01$, respectively), showing that a relative high Ang II concentration was maintained for 2 weeks (from week 6 to week 8). The Ang II level in the low-dose group was significantly increased only in week 8 ($P < 0.05$), compared to the control group.
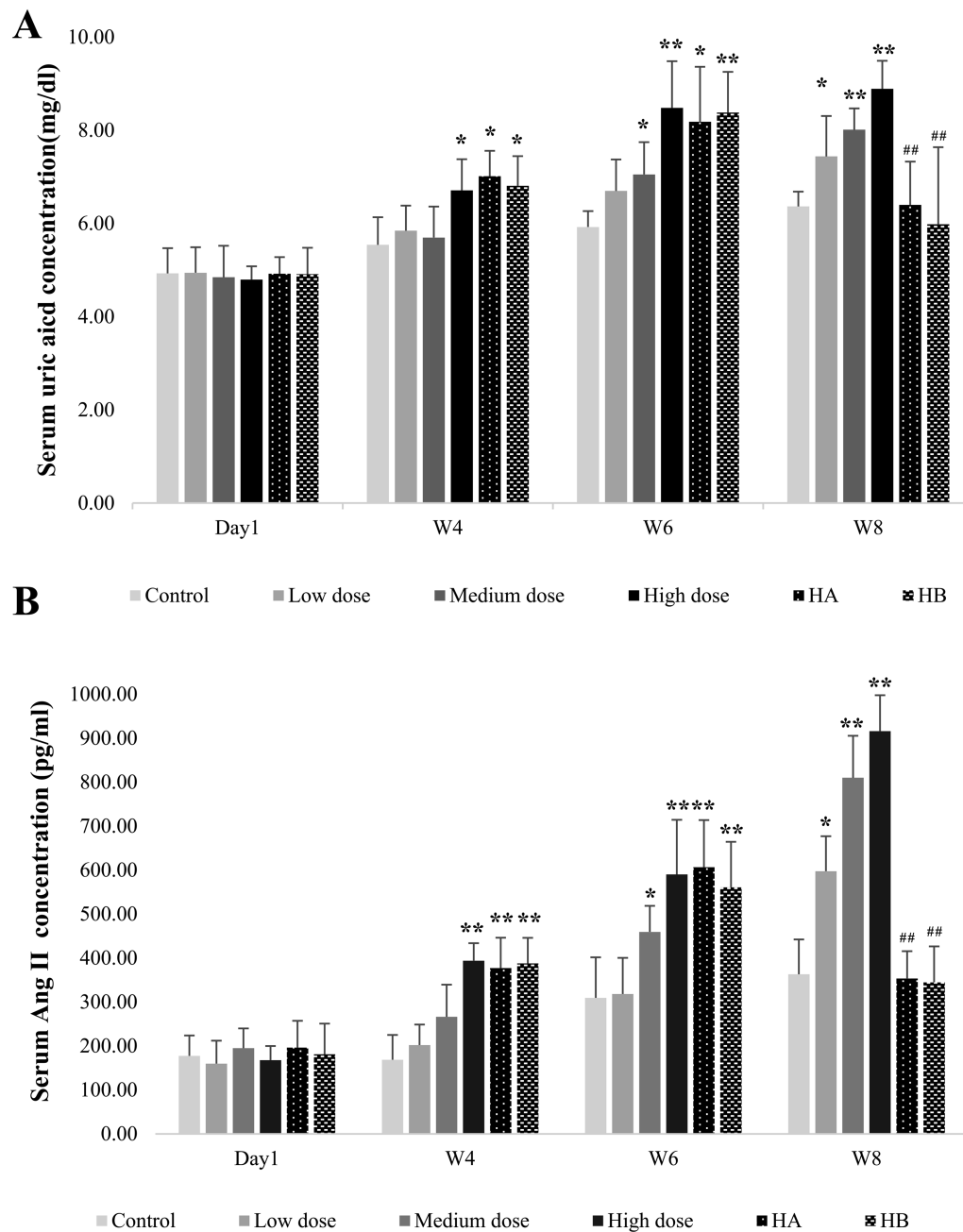
Figure 2. Hyperuricemia induction and intervention by allopurinol and benzbromarone, and ELISA measurement of serum UA and Ang II. (**A**) Serum UA concentrations in six study groups on day 1 and at the end of weeks 4, 6, and 8. (**B**) Serum angiotensin II concentrations in six study groups on day 1 and at the end of weeks 4, 6, and 8. The single star and double stars represent a significant difference compared to the control group ($P < 0.05$ and $P < 0.01$, respectively). The double pound signs represent a significant difference ($P < 0.01$) compared to the high-dose groups. The statistics were performed by the Kruskal-Wallis test and Wilcoxon test. Ang II, angiotensin II; ELISA, enzyme-linked immunosorbent assay; OA, oxonic acid potassium salt; UA, uric acid.

TABLE 1. The *P* Value of SUA Concentration in Different Groups

Group	Day 1 *P* Value (Versus Control)	Week 4 *P* Value (Versus Control)	Week 6 *P* Value (Versus Control)	Week 8 *P* Value (Versus Control)	Week 8 *P* Value (Versus High Dose Group)
Blank	—	—	—	—	—
Low	N.S.	N.S.	N.S.	<0.05	—
Medium	N.S.	N.S.	<0.05	<0.01	—
High	N.S.	<0.05	<0.01	<0.01	—
HA	N.S.	<0.05	<0.05	N.S.	<0.01
HB	N.S.	<0.05	<0.01	N.S.	<0.01

N.S., not significant.

TABLE 2. The *P* Value of Ang II Concentration in Different Groups

Group	Day 1 *P* Value (Versus Control)	Week 4 *P* Value (Versus Control)	Week 6 *P* Value (Versus Control)	Week 8 *P* Value (Versus Control)	Week 8 *P* Value (Versus High Dose Group)
Blank	—	—	—	—	—
Low	N.S.	N.S.	N.S.	<0.05	—
Medium	N.S.	N.S.	<0.05	<0.01	—
High	N.S.	<0.01	<0.01	<0.01	—
HA	N.S.	<0.01	<0.01	N.S.	<0.01
HB	N.S.	<0.01	<0.01	N.S.	<0.01

N.S., not significant.

Histopathological Analysis Revealed OS/IS Thickness Changes Under HUA

Alteration of the OS/IS is detrimental to visual function. To determine if HUA and concomitant Ang II surge have pathogenic roles in photoreceptors, we calculated the total thickness of the OS/IS in the six study groups. A significant reduction of the thickness of photoreceptor layers was found in the retinas of the hyperuricemic mice (Fig. 3A, Table 3A). Most of the damage to the photoreceptors in the low-dose group (Fig. 3B) was at 50 µm from the optic nerve head (ONH; $P < 0.05$ of the superior half; and not significant for the inferior half). Moreover, damage to the high-dose group was extended to around 150 µm ($P < 0.01$ at 50 µm, and $P < 0.05$ at 100 µm and 150 µm of the superior half, respectively; $P < 0.05$ at 50 µm, 100 µm, and 150 µm of the inferior half, respectively). In the medium-dose group, a significant reduction of thickness was found in the superior half, but only at 50 µm ($P < 0.01$). In the inferior half, the significant reduction of thickness occurred at intervals of 50 µm, 100 µm, and 150 µm ($P < 0.05$, respectively). These lesions were significantly attenuated when HUA conditions were suppressed (see Fig. 3C, Table 3A). In the HA group, significant difference was detected compared to the high-dose group ($P < 0.01$ at 50 µm, and $P < 0.05$ at 100 µm of the superior half, respectively; $P < 0.05$ at 50 µm, and $P < 0.01$ at 100 µm, and $P < 0.05$ at 150 µm of the inferior half, respectively). In the HB group, significant difference was also detected compared to the high-dose group ($P < 0.01$ at 50 µm, and $P < 0.05$ at 100 µm and 150 µm of the superior half, respectively; $P < 0.05$ at 50 µm and 100 µm of the inferior half, respectively).

As for the thickness of the PROS alone, most of the damage was in the low-dose group (Fig. 3D, Table 3B) at 50 µm from the ONH ($P < 0.05$ of the superior half; and not significant of the inferior half). The damage to the high-dose group was extended to around 150 µm ($P < 0.01$ at 50 µm, and $P < 0.05$ at 100 µm, and $P < 0.01$ at 150 µm of the superior half; $P < 0.01$ at 50 µm and 100 µm, and $P < 0.05$ at 150 µm of the inferior half). In the medium-dose group, a significant reduction of PROS thickness was found in the superior half but only at 50 µm ($p < 0.01$). In the inferior half, a significant reduction of thickness was found at intervals of 50 µm ($p < 0.01$), 100 µm, and 150 µm (both $P < 0.05$). These lesions were significantly attenuated where HUA conditions were suppressed (see Fig. 3E, Table 3B). In the HA group, significant difference was detected compared to the high-dose group ($P < 0.01$ at 50 µm and 100 µm, and $P < 0.05$ at 150 µm of the superior half; $P < 0.05$ at 50 µm, and $P < 0.01$ at 100 µm, and $P < 0.05$ at 150 µm of the inferior half). In the HB group, significant difference was also detected compared to the high-dose group ($P < 0.01$ at 50 µm, and $P < 0.05$ at 100 µm and 150 µm of the superior half;

$P < 0.05$ at 50 µm, and $P < 0.01$ at 100 µm of the inferior half).

Increased Matrix Metalloproteinase-2 Expression With HUA and Reversal Effects With Allopurinol and Benzbromarone Interventions

We found that MMP-2 expression was dose-dependent in the RGC layer (see the red arrows in Fig. 4). Little constitutive staining for MMP-2 was observed in the control and the low-dose groups. In the eyes of mice receiving the medium-dose and high-dose UA-added diet, staining for MMP-2 was markedly increased. For the HA group, the staining for MMP-2 revealed relatively weak expression compared with the high-dose group, and the expression of the HB group was almost the same as the control group.

Glial Activation With HUA

To evaluate the impact of HUA on RGCs, we performed immunostaining for GFAP, a specific marker of activated astrocytes. The fluorescent intensity of GFAP was significantly increased in the medium-dose and the high-dose groups, higher than that in the control group (both $P < 0.01$, Figs. 5A, 5B, Supplementary Table S2). The expression of GFAP in the low-dose, HA, and HB groups did not differ significantly from that in the control group. These results demonstrated that elevated SUA activated the astrocytes in the RGC layer in a dose-dependent manner, as both the HA and the HB groups had low fluorescent intensity compared to the high-dose group (both $P < 0.01$; see Fig. 5B).

HUA Disrupted the RPE Gap Junction and Caused Apoptosis

After analyzing the effect of HUA on RGCs, we asked if HUA could also damage the RPE by immunodetection of CX-43, a RPE gap junction protein (Figs. 5C, 5D, Supplementary Table S3). Low fluorescent intensity was observed in both the medium-dose and high-dose groups compared to the control group (both $P < 0.01$), whereas the HA and HB groups showed more CX-43 expression than the high-dose group (both $P < 0.01$).

After determining the detrimental effect of HUA on RPE intercellular junctions, we next conducted TUNEL assays to detect RPE apoptosis. The TUNEL-positive cells rate at all 200 µm intervals from ONH were more evident in both the medium- and high-dose groups than the control group (both $P < 0.01$; Figs. 5E, 5F, Supplementary Table S4). In contrast, compared to the high-dose group, the HA and HB groups contained fewer TUNEL-positive cells ($P < 0.05$ and
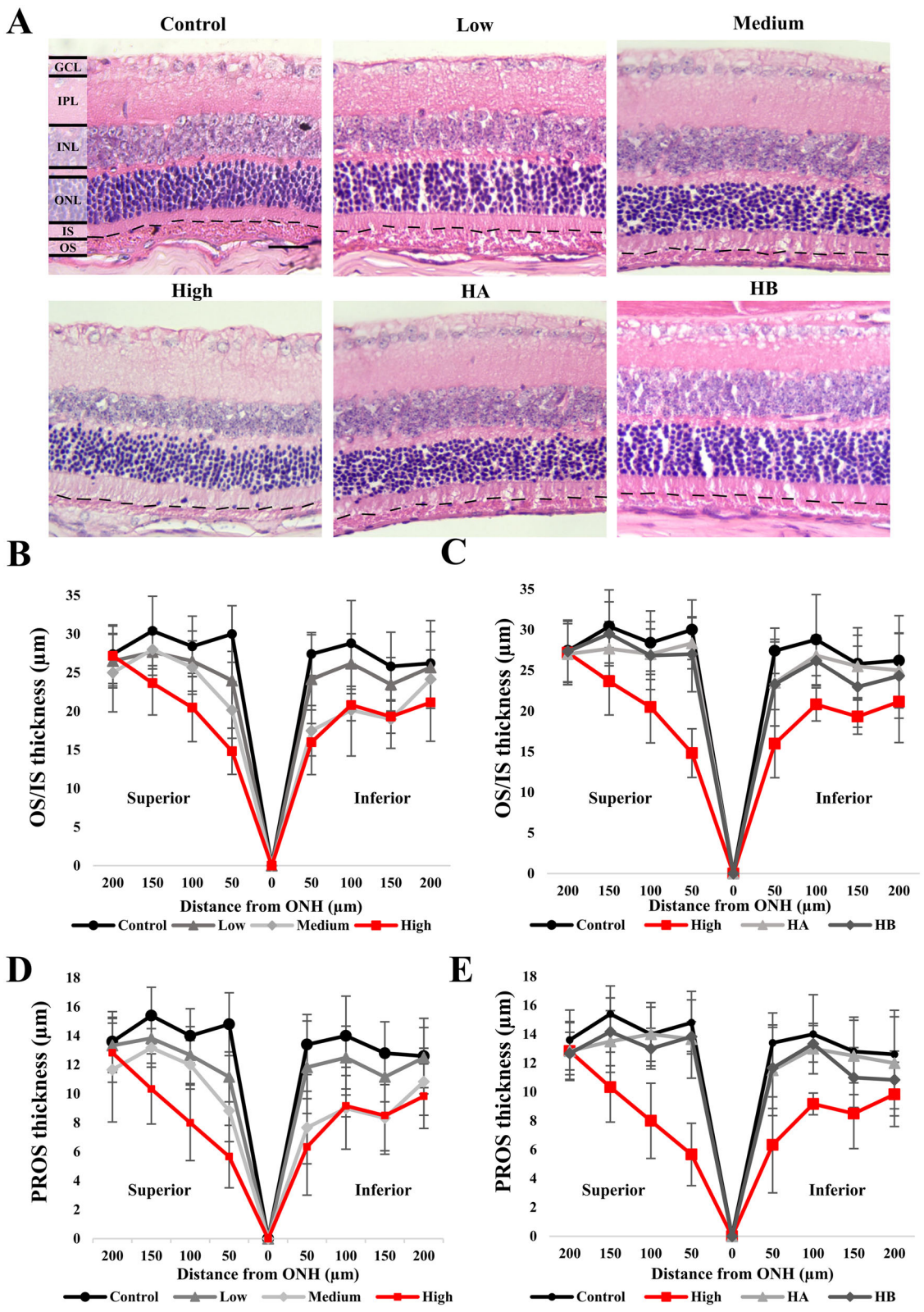
Figure 3. Histological analysis of six study groups stained with hematoxylin–eosin. (**A**) Sections stained with hematoxylin–eosin. (**B-E**) Comparison of OS/IS and PROS thickness at the end of week 8. The thickness of OS/IS and PROS was measured at 50 µm, 100 µm, 150 µm, and 200 µm intervals at superior and inferior halves to the optic nerve head. The data are presented as mean ± SD in µm. The *P* values were listed below the graphs by Wilcoxon test. The dashed lines demarcate the boundaries between OS/IS. GCL, ganglion cell layer; INL, inner nuclear layer; IPL, inner plexiform layer; OA, oxonic acid potassium salt; ONL, outer nuclear layer; OS/IS, outer segment/inner segment; UA, uric acid. Scale bar = 20 µm.

TABLE 3A. The *P* Value of OS/IS Thickness in Different Groups and Different Positions

Position/Group	200 μm *P* Value (Versus Control)	*P* Value (Versus High)	150 μm *P* Value (Versus Control)	*P* Value (Versus High)	100 μm *P* Value (Versus Control)	*P* Value (Versus High)	50 μm *P* Value (Versus Control)	*P* Value (Versus High)	50 μm *P* Value (Versus Control)	*P* Value (Versus High)	100 μm *P* Value (Versus Control)	*P* Value (Versus High)	150 μm *P* Value (Versus Control)	*P* Value (Versus High)	200 μm *P* Value (Versus Control)	*P* Value (Versus High)
Control	—	—	—	—	—	—	—	—	—	—	—	—	—	—	—	—
Low	N.S.	—	N.S.	—	N.S.	—	<0.05	—	N.S.	—	N.S.	—	N.S.	—	N.S.	—
Medium	N.S.	—	N.S.	—	N.S.	—	<0.01	—	<0.05	—	<0.05	—	<0.05	—	N.S.	—
High	N.S.	—	<0.05	—	<0.05	—	<0.01	—	<0.05	—	<0.05	—	<0.05	—	N.S.	—
HA	N.S.	N.S.	N.S.	N.S.	N.S.	<0.05	N.S.	<0.01	N.S.	<0.05	N.S.	<0.01	N.S.	<0.05	N.S.	N.S.
HB	N.S.	N.S.	N.S.	<0.05	N.S.	<0.05	N.S.	<0.01	N.S.	<0.05	N.S.	<0.05	N.S.	N.S.	N.S.	N.S.

TABLE 3B. The *P* Value of PROS Thickness in Different Groups and Different Positions

| Position/Group	200 μm *P* Value (Versus Control)	*P* Value (Versus High)	150 μm *P* Value (Versus Control)	*P* Value (Versus High)	100 μm *P* Value (Versus Control)	*P* Value (Versus High)	50 μm *P* Value (Versus Control)	*P* Value (Versus High)	50 μm *P* Value (Versus Control)	*P* Value (Versus High)	100 μm *P* Value (Versus Control)	*P* Value (Versus High)	150 μm *P* Value (Versus Control)	*P* Value (Versus High)	200 μm *P* Value (Versus Control)	*P* Value (Versus High)
Control	—	—	—	—	—	—	—	—	—	—	—	—	—	—	—	—
Low	N.S.	—	N.S.	—	N.S.	—	<0.05	—	N.S.	—	N.S.	—	N.S.	—	N.S.	—
Medium	N.S.	—	N.S.	—	N.S.	—	<0.01	—	<0.01	—	<0.05	—	<0.05	—	N.S.	—
High	N.S.	—	<0.01	—	<0.05	—	<0.01	—	<0.01	—	<0.01	—	<0.01	—	N.S.	—
HA	N.S.	N.S.	N.S.	<0.05	N.S.	<0.01	N.S.	<0.01	N.S.	<0.05	N.S.	<0.01	N.S.	<0.05	N.S.	N.S.
HB	N.S.	N.S.	N.S.	<0.05	N.S.	<0.05	N.S.	<0.01	N.S.	<0.05	N.S.	<0.01	N.S.	<0.05	N.S.	N.S.

N.S., not significant.
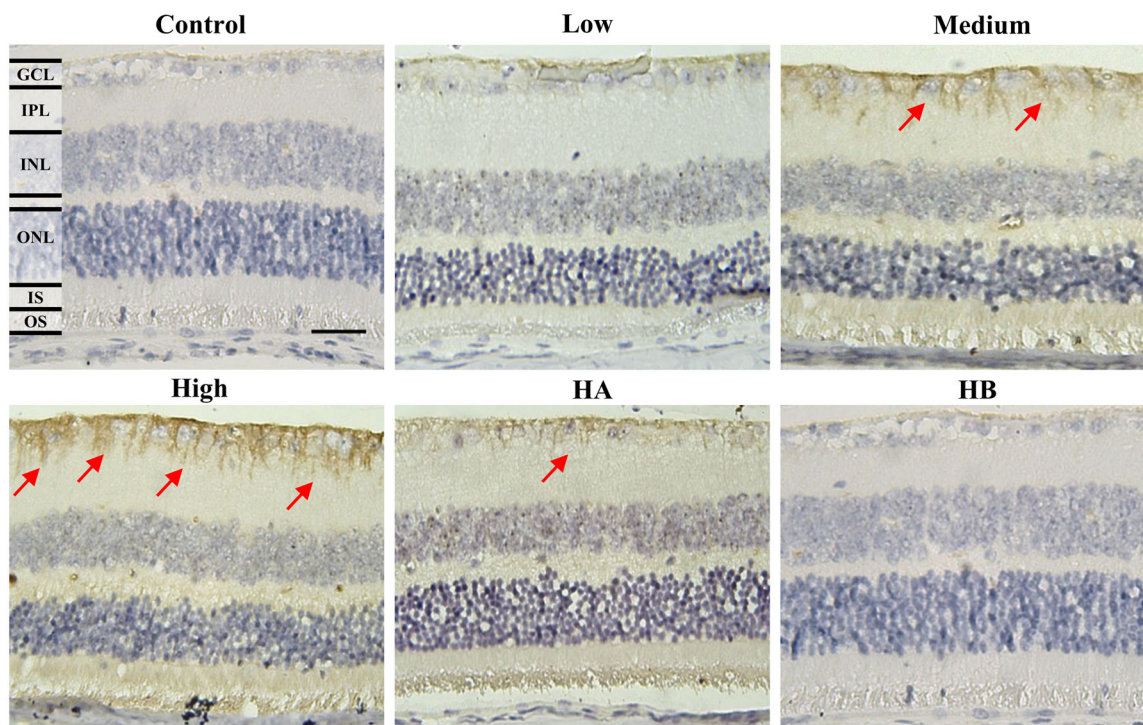
FIGURE 4. Immunohistochemical detection of MMP-2 expression in six study groups at the end of week 8. The *red arrows* indicate the MMP-2 signals (*brown color*). GCL, ganglion cell layer; INL, inner nuclear layer; IPL, outer plexiform layer; MMP-2, matrix metalloproteinase-2; ONL, outer nuclear layer; OS/IS, inner segment/outer segment. Scale bar = 20 μm.

$P < 0.01$, respectively), and almost no TUNEL-positive cells were detected in the control and the low-dose groups. The number of the apoptotic cells showed a dose-dependent manner, in compliance with the trend of SUA in different dosage groups. No TUNEL-positive cells were found in the RGC layer and the outer nuclear layer (ONL).

DISCUSSION

In the present study, we demonstrated the detrimental effects of HUA on the retina in several aspects. We showed that OS/IS total thickness and PROS thickness were decreased compared to the controls under HUA, with concomitant RAS activation, as reflected by serum Ang II elevation. We also showed that HUA leads to disruption of the gap junction and apoptosis of the RPE, as well as increased expression of MMP-2 and glial activation in the RGC layer. Most critically, our data showed the reversal effects of interventions with allopurinol or benzbromarone, providing substantial evidence that HUA is a critical causative factor for the above-observed injuries. To our knowledge, no such evidence has been reported in the literature, and these findings may permit several implications, both in basic retinal science and clinical settings.

PROS Thickness Reduction May Result From Pro-Oxidative Effects of HUA

UA is one of the water-soluble antioxidants in human plasma.[17] Physiologically, UA can remove peroxyl radicals and ROS, protecting against free-radical and oxidative damages.[18] However, UA plays a different role in intracellular environments, producing free radicals during its degradation.[19] It has been reported that UA production from xanthine generates superoxide ions, increasing oxidative stress.[20] Previous studies also indicate that UA significantly increases ROS production in adipocytes.[21] This scenario will lead to cellular injuries by high intracellular UA, as shown by the morphological damages found in the present study (see Fig. 3).

PROS is an important part of the photoreceptor structure, generally known to reflect the health of photoreceptors.[22] Reduced PROS thickness represents a major characteristic of photoreceptor injuries, resulting in impaired visual function, as exemplified in the event of branch retinal vein occlusion,[23] diabetic macular edema,[24] and idiopathic epiretinal membrane disruption.[25] In the present study, our results showed a reduction in total OS/IS (see Figs. 3B, 3C) and PROS thickness (see Figs. 3D, 3E), which indicated the retinopathogenic effect of HUA. Besides, previous studies revealed that RPE apoptosis is initiated prior to photoreceptor death.[26,27] The reduction of PROS thickness also occurred before ONL apoptosis.[22] These studies indicated that the sequence of the scenario should be followed from RPE damage, PROS thickness reduction, to ONL apoptosis, which implied a spatial relationship. In accordance with these findings reported in the previous studies, the RPE apoptosis was observed at all 200 μm intervals in the present study (see Figs. 5E, 5F), with reduced PROS thickness only found within 150 μm from ONH for the high-dose group (within 100 μm for the medium-dose group and within 50 μm for the low-dose group; see Fig. 3D). The other parts far from 200 μm from ONH actually exhibited RPE apoptosis along with normal PROS thickness. These findings may support the spatial relationship between RPE apopto-
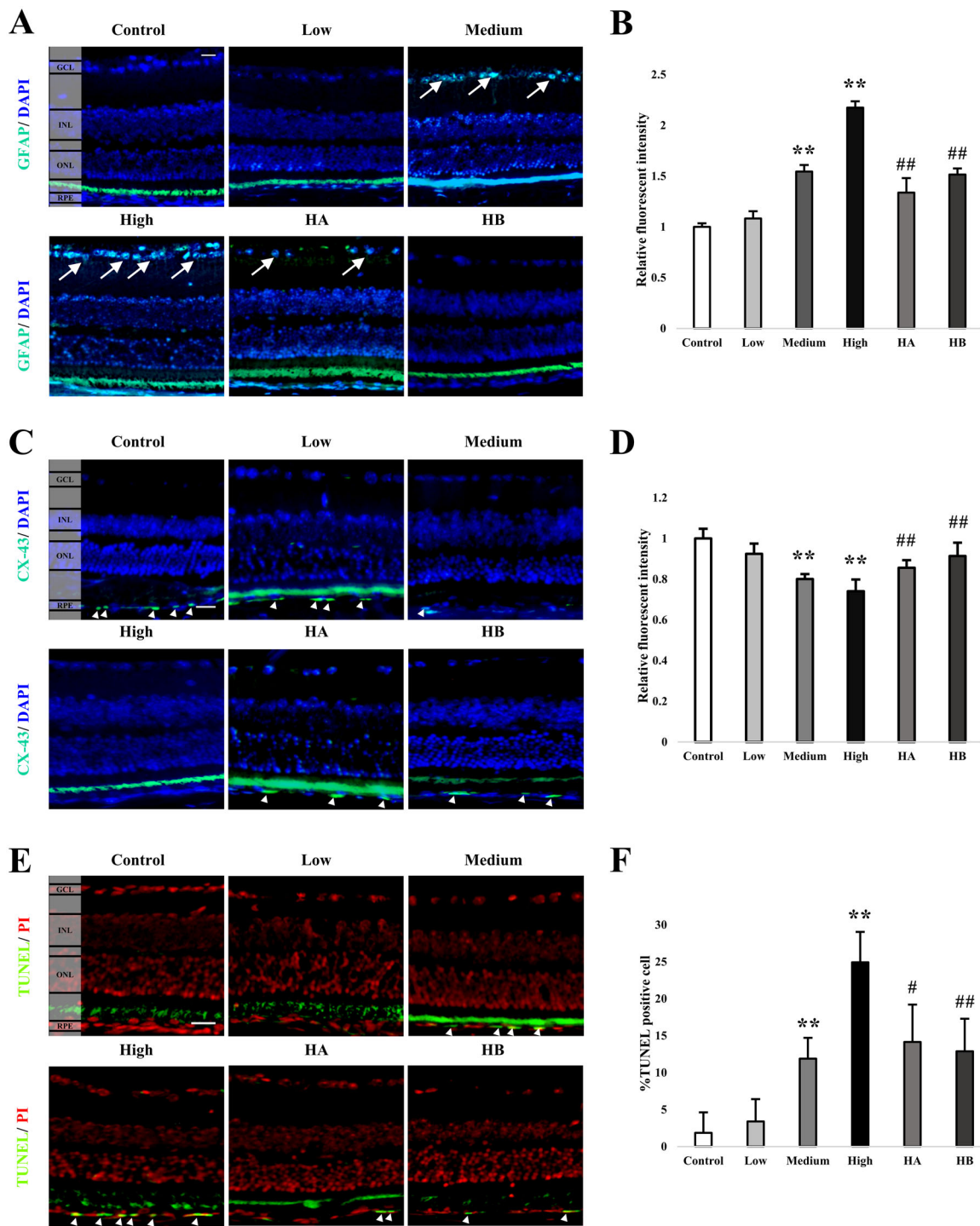
FIGURE 5. Immunofluorescent detection of GFAP, CX-43, and TUNEL. (**A, B**) GFAP detection (*white arrows*) and signal intensity comparison among six study groups at the end of week 8. (**C, D**) CX-43 detection (*white arrowheads*) and signal intensity comparison among six study groups at the end of week 8. (**E, F**) TUNEL detection (*white arrowheads*) and percentage of apoptotic cells among six study groups at the end of week 8. The photographs were analyzed for relative intensity using Image J (version 1.50f–an open-source image processing software). The significant difference was presented in single star ($P < 0.05$) and double stars ($P < 0.01$) by Wilcoxon test, compared to the control group. The significant difference was presented in single pound sign ($P < 0.05$) and double pound signs ($P < 0.01$) by Wilcoxon test, compared to the high-dose group. CX-43, connexin-43; GCL, ganglion cell layer; GFAP, glial fibrillary acidic protein; INL, inner nuclear layer; OA, oxonic acid potassium salt; ONL, outer nuclear layer; RPE, retinal pigment epithelium; TUNEL, Terminal deoxynucleotidyl-transferase-mediated deoxyuridine triphosphate-digoxigenin nick-end labeling; UA, uric acid. Scale bar = 20 µm.

sis and PROS thickness reduction. In addition, we did not find TUNEL-positive signals in ONL. Therefore, our results may indicate that the HUA-induced PROS damage was at the early stage.

From the clinical perspective, recent studies have shown that reduced PROS thickness could reflect photoreceptor degeneration prior to photoreceptor death.[22] With serous central chorioretinopathy, PROS thickness may also serve as a biomarker for the integrity of foveal photoreceptors.[28] Additionally, a recent study found that photoreceptor segment thinning was genetically associated with AMD development, serving as a potential early biomarker before RPE-Bruch's membrane complex thickening.[29] Given these findings, it may suggest that HUA could be an early indicator of retinal damage at PROS, which would potentially be applied in a clinical settings.

The Linkage Between HUA-Induced CX-43 Reduction and PROS Thickness Reduction

CX-43 is a major gap junction component responsible for communication between adjoining cells.[30] Gap junction dysregulation can start apoptosis and interrupt vascular homeostasis, which would damage intercellular transport between RPE cells.[31] Normally, RPE cells function in different aspects, including phagocytosis of PROS cell debris,[32] formation of the outer blood–retina barrier,[33] and participation in biomolecular transport.[34] RPE cells also give photoreceptors necessary nutrients and oxygen.[35] As CX-43 has been considered one of the major markers indicating RPE health,[36] the alteration of CX-43 may profoundly affect RPE cell survival, which would be a warning status of severe damage to the retina.

In this study, we found that HUA resulted in PROS thickness reduction (see Fig. 3), decreased expression of CX-43 in RPE cells (see Figs. 5C, 5D), and increase of RPE cell apoptosis (see Figs. 5E, 5F). These results were all reversed through intervention with either allopurinol or benzbromarone, two commonly prescribed drugs for HUA treatment. Therefore, we deduced that the whole HUA-induced pathology may start from RPE cell malfunction, as our data supported a spatial relationship between RPE apoptosis and PROS thickness reduction according to the administered UA dose. The destruction of CX-43 by HUA decreased the communication between RPE cells, resulting in the elevated apoptosis. After that, RPE cells lose the ability to remove waste materials and cannot maintain photoreceptor functions. Finally, the condition of RPE and photoreceptors deteriorate, laying a foundation for the HUA-induced etiopathogenic mechanism.

Detrimental Effects of the Activation of the RAS on RPE

RAS is classically regarded as a blood pressure regulator. However, emerging evidence revealed that RAS is also contributed to regulate inflammatory response.[37] Recent studies found that HUA has been associated with RAS activation, with the elevation of its main components including (pro)renin, Ang II, and angiotensin type 1 receptor.[11] Most RAS components, including angiotensin-converting enzymes, were also found to be locally expressed in many tissues, including the retina. This may indicate that peripheral tissues have the ability to produce Ang II and locally exert its effect.[38,39] Being the main effector in RAS, Ang

II serves as a key driver of various diseases and multiple physiological changes in the retina. The impact of Ang II elevation is to break down the RPE basement membrane, which is involved in retinal injuries.[40] Furthermore, Ang II can induce the upregulation of vascular endothelial growth factor receptor-2 (VEGFR-2) and potentiate related angiogenetic activities in retinal endothelial cells, manifesting the significance of RAS in the pathogenesis of retinal diseases.[41] In the present study, our data further elucidated the influence of HUA on RAS activation by showing Ang II elevation in the HUA animal model. Adding to previous knowledge of HUA's influence on Ang II, which would lead to retinal damages, our data showed that the detrimental effects of HUA could be reversed by intervention with allopurinol or benzbromarone (see Fig. 2B). These findings indicated that HUA-induced retinal injuries may be triggered through RAS.

Increased MMP-2 Expression in RGCs and its Aftermath

We also observed an increased expression of MMP-2 in RGCs (see Fig. 4). In a previous report, MMP-2 was found positively correlated with the regeneration of RGC axons in a rat model.[42] Inhibition of MMP has also been reported to reduce the outgrowth and guidance of RGC axons. These findings implied a positive effect of MMPs in axonal regeneration.[43] Arguably, the expression of MMPs, especially MMP-2 and MMP-9, is responsible for the degradation of extracellular matrix (ECM) protein in Bruch's membrane and the RPE basement membrane.[40] Altered expression of MMPs may interrupt intercellular and cell–ECM interactions, which aids the formation of drusen and increases the risk of choroidal endothelial cell invasion.[44] MMPs also play critical roles in ECM remodeling at ONH, thereby predisposing RGCs to damage.[45] For example, MMP-induced proteolysis leads to the loss of the cell–ECM connection through which retinal degeneration can progress.[46] Our data demonstrated that MMP-2 expression was significantly higher in the high-dose group than the others, with reversal effects by allopurinol or benzbromarone treatments (see Fig. 4). This dose-dependent effect supports the pathogenic linkage between HUA and MMP-2, implying excessive ECM protein remodeling in RGCs. Although no damage to RGCs was observed, our findings may potentially predispose a status of RGCs injuries under HUA.

Glial Activation Under HUA Influence

The effects of glial activation on the retina, as shown by GFAP expression, remain under debate. Both positive and negative aspects have been identified. On the negative side, excessive GFAP expression has been known to occur when the retina is injured, likely in an inhibitory environment that would eventually deter axon regeneration after neuron damage.[47] Abnormal increases of GFAP expression in RGCs were considered a response to oxidative stress.[48] Higher GFAP expression also increases cell stiffness, which would hinder axonal regeneration due to the unfavorable milieu for the growth of neurites.[49] However, on the positive side, both reactive Müller cells and retinal astrocytes generate trophic factors to RGCs after injury.[50,51] Müller glia activation also has been regarded as a compensatory response to promote the viability of RGCs.[52] In fact, some trophic factors enhance
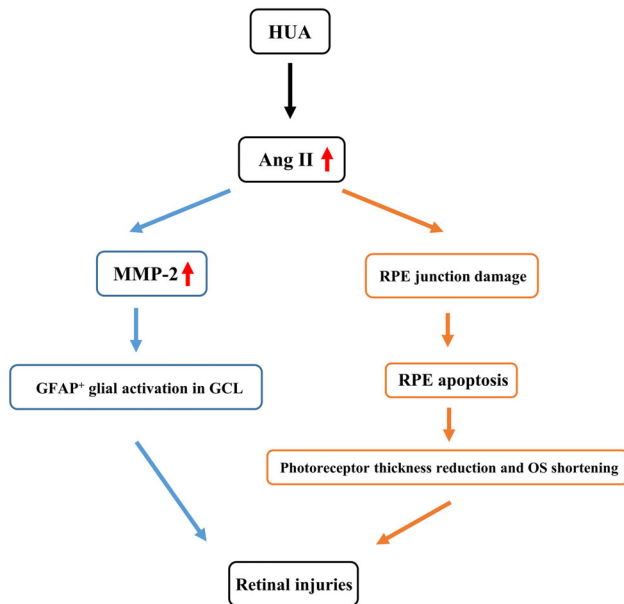
Figure 6. Summary of HUA-induced pathogenesis leading to early AMD or relevant retinopathy. AMD, age-related macular degeneration; Ang II, angiotensin II; GCL, ganglion cell layer; HUA, hyperuricemia; OS, outer segment; RGC, retina ganglion cell; RPE, retinal pigment epithelium.

cell survival, whereas others may promote optimal regeneration of RGCs through axonal growth.[53]

The present study found that GFAP expression was significantly increased in the high-dose group, and it was reversed in the HA and HB groups (see Figs. 5A, 5B). Previous studies found that acute glial activation is neuroprotective, whereas the sustained activity of glial cells is regarded as detrimental, partially because of the release of inflammatory cytokines.[46] Moreover, the RGC survival promoted by glial activation is transient, which is not necessarily corresponding to the axonal revitalization.[53] As HUA is a major contributor to the development or progression of chronic kidney disease with several inflammatory cytokines,[8] the high expression of GFAP with long-term HUA in the present study should also be regarded as harmful to the RGCs. Therefore, consistent with the perspectives of previous literature, we considered that HUA might contribute to the abnormal activation of RGCs.

Implication of HUA in Retinal Diseases

Based on our dose-dependent and cause-and-effect findings, we proposed two possible routes from HUA to retinal damage (see Fig. 6). HUA may be the onset initiator to induce damage to the RPE junction, presumably leading to RPE apoptosis. The death of RPE cells impedes the supply and maintenance of PROS, and leads to the destruction in the photoreceptor as reflected by PROS thickness reduction. Another route may be that HUA triggers the RAS pathway, resulting in a surge of Ang II and subsequent elevation of MMP-2 expression in RGCs. With interruption of cell-cell interaction, the retinal damage may thereby progress. In response, the abnormal glial activation would occur, suggesting a detrimental effect by HUA. No matter which route it might be, the HUA-induced elevation of Ang II posed a threat to the retina without restraint to PROS, RPE, or RGCs. This "systematic" characteristic indicated that the effect of RAS activation may be elusive between all the above-mentioned retinal components.

For specific ocular diseases, we found increased MMP-2 expression in RGCs, which is proved to associate with glaucomatous optic neuropathy.[54] The higher GFAP expression may be another evidence, as microglial activation is a typical glaucoma feature subsequent to elevated intraocular pressure and ischemia.[55] Measurement of intraocular pressure change and the retina functional test should be performed in future studies for verification.

As for our hypothesis that "hyperuricemic AMD" may exist, it is still inconclusive whether HUA is directly related to AMD, as we did not find any typical AMD hallmarks, such as geographic atrophy and drusen. However, we indeed found that PROS thickness was reduced, which was recently regarded as an indicator of early AMD pathology.[26] We also found that HUA-induced retinal damage was concentrated in RPE cells, as reflected by higher TUNEL signals and decreased CX-43 expression. In previous studies, RAS activation in RPE cells was found to initiate the induction of tumor necrosis factor-α, interleukin-6 (IL-6), and IL-1β, which were considered as choroidal neovascularization inducers.[38,56] Besides, the NLRP3 inflammasome, which is activated in HUA by monosodium urate crystal, is proved to exist in RPE and is triggered by lipofuscin and drusen.[56,57] Increased SUA level was also positively associated with the concentration of lipid profiles, indicating an anomalous lipid metabolic status.[58] With abnormal lipid accumulation, drusen may thereby be deposited, leading to AMD development.[59] In conclusion, the existence of "hyperuricemic AMD" needs more investigations, but our findings may provide some hints about the role of HUA in AMD.

Limitations

In the present study, several structural analyses were conducted to investigate the impact of HUA on retina. However, one of the limitations was lack of a functional test and evidence with electron microscopy, which warrants further investigations to link HUA to specific ocular diseases. In addition, the HUA condition was maintained just for 4 weeks in the high-dose group, which left some questions needed to be answered. For example, whether an abortion of an HUA diet after 6 weeks would result in a regression of retinal changes even without SUA lowering treatment should be investigated. Besides, whether the absence of geographic atrophy and drusen was due to insufficient duration of HUA needs to be confirmed. Future experiments with different study periods may further elucidate the detrimental effects of HUA on the retina. In addition, because not all patients with HUA developed eye diseases, such as AMD and glaucoma, a more detailed investigation on molecular pathogenesis or epidemiology should be conducted. Another limitation was that the exact role of Ang II in HUA-induced retinal damage needs further elucidation. For example, Ang II inhibitors may be administered to revert the lesions in the GCL and RPE.

More importantly, our data indicated that UA lowering agents, allopurinol and benzbromarone, have ameliorated the HUA-induced retinal damages. This finding would be of great significance to clinical retinologists in that the control of SUA is critical for retinal health.

CONCLUSION

In the present study, we conducted several experiments to confirm the risk of HUA. We found that HUA may be a causative factor for retinal damages and the adverse effects can be reversed by SUA lowering agents.

Author contributions: H.-L.P. designed and performed the experiments, analyzed data, and wrote the paper. S.M.-T.H., Y.-S.S., and X.-Y.S. performed experiments and analyzed the data. H.-H.C. contributed to designing the project, data interpretation, and writing sections of the manuscript. D.P.-C.L. conceived and designed the project, designed all experiments, analyzed data, and wrote the paper.

Disclosure: **H.-L. Pai**, None; **S.M.-T. Hsieh**, None; **Y.-S. Su**, None; **X.-Y. Sue**, None; **H.-H. Chang**, None; **D.P.-C. Lin**, None

References

1. Hirode G, Wong RJ. Trends in the Prevalence of Metabolic Syndrome in the United States, 2011–2016. *JAMA*. 2020;323:2526–2528.

2. Grundy SM, Cleeman JI, Daniels SR, et al. Diagnosis and Management of the Metabolic Syndrome. *Circulation*. 2005;112:2735–2752.

3. Poh S, Mohamed Abdul RB, Lamoureux EL, Wong TY, Sabanayagam C. Metabolic syndrome and eye diseases. *Diabetes Res Clin Pract*. 2016;113:86–100.

4. Karasik A, Modan M, Halkin H, Treister G, Fuchs Z, Lusky A. Senile cataract and glucose intolerance: the Israel Study of glucose Intolerance Obesity and Hypertension (The Israel GOH Study). *Diabetes Care*. 1984;7:52–56.

5. Raman R, Pal SS, Adams JSK, Rani PK, Vaitheeswaran K, Sharma T. Prevalence and Risk Factors for Cataract in Diabetes: Sankara Nethralaya Diabetic Retinopathy Epidemiology and Molecular Genetics Study, Report No. 17. *Invest Ophthalmol Vis Sci*. 2010;51:6253–6261.

6. Sivaprasad S, Gupta B, Crosby-Nwaobi R, Evans J. Prevalence of Diabetic Retinopathy in Various Ethnic Groups: A Worldwide Perspective. *Survey of Ophthalmol*. 2012;57:347–370.

7. Ghaem Maralani H, Tai BC, Wong TY, et al. Metabolic syndrome and risk of age-related macular degeneration. *Retina*. 2015;35:459–466.

8. Dalbeth N, Choi HK, Joosten LAB, et al. Gout. *Nat Rev Dis Primers*. 2019;5:69.

9. Shen S, He F, Cheng C, Xu B, Sheng J. Uric acid aggravates myocardial ischemia-reperfusion injury via ROS/NLRP3 pyroptosis pathway. *Biomed Pharmacother*. 2021;133:110990.

10. Yu MA, Sánchez-Lozada LG, Johnson RJ, Kang DH. Oxidative stress with an activation of the renin-angiotensin system in human vascular endothelial cells as a novel mechanism of uric acid-induced endothelial dysfunction. *J Hypertens*. 2010;28:1234–1242.

11. Zhang J, Lin X, Xu J, Tang F. Apelin-13 reduces oxidative stress induced by uric acid via downregulation of renin-angiotensin system in adipose tissue. *Toxicol Lett*. 2019;305:51–57.

12. Pai H-L, Chang H-H, Lin DP-C. The need to investigate hyperuricemia as a factor in the onset of age-related macular degeneration. *Eye*. 2021;35:1804–1807.

13. Subramani S, Khor SE, Livingstone BI, Kulkarni UV. Serum uric acid levels and its association with age-related macular degeneration (ARMD). *Med J Malaysia*. 2010;65:36–40.

14. Singh JA, Cleveland JD. Gout and the risk of age-related macular degeneration in the elderly. *PLoS One*. 2018;13:e0199562.

15. Schneider CA, Rasband WS, Eliceiri KW. NIH Image to ImageJ: 25 years of image analysis. *Nature Methods*. 2012;9:671–675.

16. Jensen EC. Quantitative Analysis of Histological Staining and Fluorescence Using ImageJ. *Anatomic Record*. 2013;296:378–381.

17. Fabbrini E, Serafini M, Colic Baric I, Hazen SL, Klein S. Effect of plasma uric acid on antioxidant capacity, oxidative stress, and insulin sensitivity in obese subjects. *Diabetes*. 2014;63:976–981.

18. Ames BN, Cathcart R, Schwiers E, Hochstein P. Uric acid provides an antioxidant defense in humans against oxidant- and radical-caused aging and cancer: a hypothesis. *Proc Natl Acad Sci USA*. 1981;78:6858–6862.

19. Lin KM, Lu CL, Hung KC, et al. The Paradoxical Role of Uric Acid in Osteoporosis. *Nutrients*. 2019;11:2111–2127.

20. Berry CE, Hare JM. Xanthine oxidoreductase and cardiovascular disease: molecular mechanisms and pathophysiological implications. *J Physiol*. 2004;555:589–606.

21. Atashi F, Modarressi A, Pepper MS. The role of reactive oxygen species in mesenchymal stem cell adipogenic and osteogenic differentiation: a review. *Stem Cells Dev*. 2015;24:1150–1163.

22. Nagai N, Minami S, Suzuki M, et al. Macular Pigment Optical Density and Photoreceptor Outer Segment Length as Predisease Biomarkers for Age-Related Macular Degeneration. *J Clin Med*. 2020;9:1347–1356.

23. Shiono A, Kogo J, Sasaki H, et al. Optical coherence tomography findings as a predictor of clinical course in patients with branch retinal vein occlusion treated with ranibizumab. *PLoS One*. 2018;13:e0199552.

24. Kogo J, Shiono A, Sasaki H, et al. Foveal Microstructure Analysis in Eyes with Diabetic Macular Edema Treated with Vitrectomy. *Adv Ther*. 2017;34:2139–2149.

25. Shiono A, Kogo J, Klose G, et al. Photoreceptor outer segment length: a prognostic factor for idiopathic epiretinal membrane surgery. *Ophthalmology*. 2013;120:788–794.

26. Chen C, Cano M, Wang JJ, et al. Role of unfolded protein response dysregulation in oxidative injury of retinal pigment epithelial cells. *Antioxid Redox Signal*. 2014;20:2091–2106.

27. Moriguchi M, Nakamura S, Inoue Y, et al. Irreversible Photoreceptors and RPE Cells Damage by Intravenous Sodium Iodate in Mice Is Related to Macrophage Accumulation. *Invest Ophthalmol Vis Sci*. 2018;59:3476–3487.

28. Hasegawa T, Okamoto M, Masuda N, Ueda T, Ogata N. Relationship between foveal microstructures and visual outcomes in eyes with resolved central serous chorioretinopathy. *Graefes Arch Clin Exp Ophthalmol*. 2015;253:343–350.

29. Zekavat SM, Sekimitsu S, Ye Y, et al. Photoreceptor Layer Thinning Is an Early Biomarker for Age-Related Macular Degeneration: Epidemiologic and Genetic Evidence from UK Biobank OCT Data. *Ophthalmology*. 2022;129:694–707.

30. Lampe PD, Lau AF. The effects of connexin phosphorylation on gap junctional communication. *Int J Biochem Cell Biol*. 2004;36:1171–1186.

31. Hutnik CML, Pocrnich CE, Liu H, Laird DW, Shao Q. The Protective Effect of Functional Connexin43 Channels on a Human Epithelial Cell Line Exposed to Oxidative Stress. *Invest Ophthalmol Vis Sci*. 2008;49:800–806.

32. Naso F, Intartaglia D, Falanga D, et al. Light-responsive microRNA miR-211 targets Ezrin to modulate lysosomal biogenesis and retinal cell clearance. *Embo J*. 2020;39:e102468.

33. Kuo C, Green CR, Rupenthal ID, Mugisho OO. Connexin43 hemichannel block protects against retinal pigment epithelial cell barrier breakdown. *Acta Diabetol*. 2020;57:13–22.

34. Khristov V, Wan Q, Sharma R, Lotfi M, Maminishkis A, Bharti K. Polarized Human Retinal Pigment Epithelium Exhibits Distinct Surface Proteome on Apical and Basal Plasma Membranes. *Methods Mol Biol*. 2018;1722:223–247.

35. Tokarz P, Piastowska-Ciesielska AW, Kaarniranta K, Blasiak J. All-Trans Retinoic Acid Modulates DNA Damage Response and the Expression of the VEGF-A and MKI67 Genes in ARPE-19 Cells Subjected to Oxidative Stress. *Intl J Molecul Sci*. 2016;17:898.

36. Hoang QV, Qian H, Ripps H. Functional analysis of hemichannels and gap-junctional channels formed by connexins 43 and 46. *Mol Vis*. 2010;16:1343–1352.

37. Satou R, Penrose H, Navar LG. Inflammation as a Regulator of the Renin-Angiotensin System and Blood Pressure. *Curr Hypertens Rep*. 2018;20:100.

38. Kurihara T, Ozawa Y, Ishida S, Okano H, Tsubota K. Renin-Angiotensin system hyperactivation can induce inflammation and retinal neural dysfunction. *Int J Inflam*. 2012;2012:581695.

39. Soubrier F, Alhenc-Gelas F, Hubert C, et al. Two putative active centers in human angiotensin I-converting enzyme revealed by molecular cloning. *Proc Natl Acad Sci USA*. 1988;85:9386–9390.

40. Pons M, Cousins SW, Alcazar O, Striker GE, ME Marin-Castaño. Angiotensin II-induced MMP-2 activity and MMP-14 and basigin protein expression are mediated via the angiotensin II receptor type 1-mitogen-activated protein kinase 1 pathway in retinal pigment epithelium: implications for age-related macular degeneration. *Am J Pathol*. 2011;178:2665–2681.

41. Otani A, Takagi H, Oh H, et al. Angiotensin II–Stimulated Vascular Endothelial Growth Factor Expression in Bovine Retinal Pericytes. *Invest Ophthalmol Vis Sci*. 2000;41:1192–1199.

42. Ahmed Z, Dent RG, Leadbeater WE, Smith C, Berry M, Logan A. Matrix metalloproteases: degradation of the inhibitory environment of the transected optic nerve and the scar by regenerating axons. *Mol Cell Neurosci*. 2005;28:64–78.

43. Gaublomme D, Buyens T, De Groef L, et al. Matrix metalloproteinase 2 and membrane type 1 matrix metalloproteinase co-regulate axonal outgrowth of mouse retinal ganglion cells. *J Neurochem*. 2014;129:966–979.

44. De Groef L, Van Hove I, Dekeyster E, Stalmans I, Moons L. MMPs in the neuroretina and optic nerve: modulators of glaucoma pathogenesis and repair? *Invest Ophthalmol Vis Sci*. 2014;55:1953–1964.

45. Akhter N, Nix M, Abdul Y, Singh S, Husain S. Delta-opioid receptors attenuate TNF-α-induced MMP-2 secretion from human ONH astrocytes. *Invest Ophthalmol Vis Sci*. 2013;54:6605–6611.

46. Vecino E, Rodriguez FD, Ruzafa N, Pereiro X, Sharma SC. Glia–neuron interactions in the mammalian retina. *Prog Retin Eye Res*. 2016;51:1–40.

47. Toops KA, Hagemann TL, Messing A, Nickells RW. The effect of glial fibrillary acidic protein expression on neurite outgrowth from retinal explants in a permissive environment. *BMC Res Notes*. 2012;5:693.

48. Barber AJ, Antonetti DA, Gardner TW. Altered expression of retinal occludin and glial fibrillary acidic protein in experimental diabetes. The Penn State Retina Research Group. *Invest Ophthalmol Vis Sci*. 2000;41:3561–3568.

49. Bringmann A, Wiedemann P. Müller Glial Cells in Retinal Disease. *Ophthalmologica*. 2012;227:1–19.

50. Kinkl N, Ruiz J, Vecino E, Frasson M, Sahel J, Hicks D. Possible involvement of a fibroblast growth factor 9 (FGF9)–FGF receptor-3-mediated pathway in adult pig retinal ganglion cell survival in vitro. *Mol Cell Neurosci*. 2003;23:39–53.

51. Bonnet D, Garcia M, Vecino E, Lorentz J-G, Sahel J, Hicks D. Brain-derived neurotrophic factor signalling in adult pig retinal ganglion cell neurite regeneration in vitro. *Brain Research*. 2004;1007:142–151.

52. Zucchiatti I, Parodi MB, Pierro L, et al. Macular Ganglion Cell Complex and Retinal Nerve Fiber Layer Comparison in Different Stages of Age-Related Macular Degeneration. *Am J Ophthalmol*. 2015;160:602–607.e601.

53. Vecino E, Garcıá-Grespo D, Garcıá M, Martinez-Millán L, Sharma SC, Carrascal E. Rat retinal ganglion cells co-express brain derived neurotrophic factor (BDNF) and its receptor TrkB. *Vis Res*. 2002;42:151–157.

54. Yan X, Tezel G, Wax MB, Edward DP. Matrix metalloproteinases and tumor necrosis factor alpha in glaucomatous optic nerve head. *Arch Ophthalmol*. 2000;118:666–673.

55. Wang L, Cioffi GA, Cull G, Dong J, Fortune B. Immunohistologic Evidence for Retinal Glial Cell Changes in Human Glaucoma. *Invest Ophthalmol Vis Sci*. 2002;43:1088–1094.

56. Kauppinen A, Paterno JJ, Blasiak J, Salminen A, Kaarniranta K. Inflammation and its role in age-related macular degeneration. *Cell Mol Life Sci*. 2016;73:1765–1786.

57. Pan C, Banerjee K, Lehmann GL, et al. Lipofuscin causes atypical necroptosis through lysosomal membrane permeabilization. *Proc Natl Acad Sci USA*. 2021;118:e21001221181–e21001221211.

58. Ali N, Rahman S, Islam S, et al. The relationship between serum uric acid and lipid profile in Bangladeshi adults. *BMC Cardiovasc Disord*. 2019;19:42.

59. Ebrahimi KB, Handa JT. Lipids, lipoproteins, and age-related macular degeneration. *J Lipids*. 2011;2011:802059.